

New Low Surface Brightness Dwarf Galaxies Detected Around Nearby Spirals

I. D. Karachentsev,^{1,*} P. Riepe,² T. Zilch,² M. Blauensteiner,² M. Elvov,²
 P. Hochleitner,² B. Hubl,² G. Kerschhuber,² S. Küppers,² F. Neyer,² R. Pözl,²
 P. Rimmel,² O. Schneider,² R. Sparenberg,² U. Trulson,² G. Willems,² and H. Ziegler²

¹*Special Astrophysical Observatory of the Russian AS, Nizhnij Arkhyz 369167, Russia*
²*Tief Belichtete Galaxien group of Vereinigung der Sternfreunde e.V., Fachgruppe Astrofotografie,
 Heppenheim, D-64629 Germany*

(Received June 22, 2015; Revised July 31, 2015)

We conduct a survey of low surface brightness (LSB) satellite galaxies around the Local Volume massive spirals using long exposures with small amateur telescopes. We identified 27 low and very low surface brightness objects around the galaxies NGC 672, 891, 1156, 2683, 3344, 4258, 4618, 4631, and 5457 situated within 10 Mpc from us, and found nothing new around NGC 2903, 3239, 4214, and 5585. Assuming that the dwarf candidates are the satellites of the neighboring luminous galaxies, their absolute magnitudes are in the range of $-8.6 > M_B > -13.3$, their effective diameters are 0.4–4.7 kpc, and the average surface brightness is $26^m/1/\square''$. The mean linear projected separation of the satellite candidates from the host galaxies is 73 kpc. Our spectroscopic observations of two LSB dwarfs with the Russian 6-meter telescope confirm their physical connection to the host galaxies NGC 891 and NGC 2683.

1. INTRODUCTION

The two past decades witnessed the rapid formation of a new direction in extragalactic astronomy, called the cosmology of the nearby universe. This is facilitated by the ongoing wide-field surveys of the northern and southern sky in the optical, infrared, and radio ranges [1–9], which allowed astronomers to detect a lot of dwarf galaxies and to measure their radial velocities [10–12]. Accurate bulk measurements of distances to nearby galaxies carried out with the Hubble Space Telescope are also a significant advancement factor. According to the latest observational data report, titled the *Updated Nearby Galaxy Catalog* (UNGC) [13], the surrounding volume around the Milky Way with a radius of about 10 Mpc contains about nine hundred galaxies, the majority of which have their distances and radial velocities measured, and stellar masses, star formation rates, and other basic characteristics determined. The generally accessible database of observational data on the galaxies of the Local Volume [14] (<http://www.sao.ru/1v/1vgdb/>) is regularly updated with new objects. About 85% of the UNGC [13] sample are dwarf galaxies whose integrated luminosity is lower than that of the Magellanic Clouds.

The numerical simulations of the large-scale structure of the Universe performed on super-

computers within the standard Λ CDM cosmological model [15, 16] revealed a huge discrepancy in the observed number of dwarf galaxies relative to their number expected within the standard model. The observed number of dwarf satellites around nearby high luminosity galaxies turned out to be ten times smaller than expected. This as yet unexplained situation was called the “missing satellites” paradox. An ad hoc search for dwarf galaxies around the nearest massive galaxies M 31 [17–19] and M 81 [20, 21] has only partially alleviated this paradox. Therefore, a further in-depth search for yet fainter dwarf systems continues to be a topical task of observational cosmology of the nearby universe.

According to theoretical and observational data, the integrated luminosity of a galaxy L is proportional to the cube of its effective linear diameter A . This implies that the average luminosity density of galaxies L/A^3 is about the same regardless of their size, however, their average surface brightness L/A^2 drops with decreasing linear diameter of the galaxy. For this reason the smallest dwarf satellites are to be searched for among LSB objects. Medium-sized amateur telescopes (about 0.3 m in diameter) with a focal ratio $f/D \sim 4\text{--}8$ and equipped with CCD detectors can be used for this task. The images obtained on such telescopes with exposures of about 10 hours reveal quite well objects with the surface brightness $SB \sim 27^m\text{--}28^m/\square''$ and angular sizes exceeding $0'.2$, which roughly corresponds to the typical parameters of dwarf galaxies located within the Local Volume.

* Electronic address: ikar@sao.ru

According to preliminary estimates, the UNGC is about 50% complete for the galaxies with the absolute magnitude M_B brighter than -11^m0 and the surface brightness $SB < 26^m/\square''$. The characteristic linear diameter of dwarf galaxies near the 50% limit is about 1 kpc, which corresponds to an angular size $a \sim 0'.3$ at the far edge of the Local Volume. Therefore, hours-long exposures of the vicinity of nearby bright galaxies with modern amateur telescopes allow successful detection of new dwarf satellites around them. Such a systematic observational program provides an independent opportunity to clarify the extent of completeness of the UNGC in terms of the luminosity of dwarf galaxies, their linear dimensions and surface brightnesses.

2. TBG GROUP OBSERVATIONAL PROJECT

The TBG (Tief Belichtete Galaxien) group deals with very long exposure images of galaxies made using amateur telescopes of medium caliber. The group was organized by P. Riepe in January 2012 in the *Astrophotography* department of the German association VdS (Vereinigung der Sternfreunde e.V.). Now the group consists of about 30 astrophotographers from Germany, Austria, and Switzerland, equipped with 10 to 110 cm diameter telescopes. Some TBG telescopes are located in the United States and Spain and are remotely operated. The entire project is coordinated by P. Riepe and T. Zilch. For deep-sky images, reaching $SB \sim 28^m/\square''$, the group uses high-quality CCD detectors and data reduction packages which include the dark frame subtraction, flat field correction, and calibration procedures.

One of the main tasks of the TBG group is photographing the neighborhoods of nearby bright galaxies to look for LSB dwarf satellites around them. The program includes more than 50 galaxies of sufficiently high luminosity located within a distance of 10 Mpc. Exposure time with broadband filters varied depending on weather conditions. The typical exposure lasted from 10 to 15 hours, though in some cases it reached up to 50 hours.

After the necessary image processing steps and contrasting of the images, we conducted a visual search for low and very low surface brightness objects, focusing on the average characteristics of the known satellites of the Milky Way

and Andromeda (M 31).

Below we present the results of the satellite candidate search around thirteen nearby spiral galaxies, obtained in implementing the initial phase of this program. The following articles of this series will present the results of monitoring the neighborhoods of still about 40 massive galaxies in the Local Volume.

3. FIRST-SEASON OBSERVATIONS

3.1. NGC 4631

This late-type spiral galaxy, seen edge-on, is the brightest representative of a scattered group, which includes about 30 members. The distance to it, $D = 7.38$ Mpc, was measured by Radburn-Smith et al. [22] from the luminosity of red giant branch stars. Another bright spiral galaxy, NGC 4656, is located at an angular distance of $32'$ south of NGC 4631. Both of them have structural distortions which are obviously caused by mutual gravitational perturbations.

In spring 2013, several TBG group members have obtained the images of NGC 4631 and its environs with a total exposure of 24^h . Methodological details of these observations were given earlier [23]. We marked three very low surface brightness dwarf galaxies in the combined image, dw1, dw2, dw3, as well as a tidal strip that stretches from NGC 4631 to the northwest through dw1 and to the southeast towards the galaxy NGC 4656. The presence of this tidal strip was later confirmed by Martinez-Delgado et al. [24]. In February 2013 and March 2014, F. Neyer obtained new, deeper images of the NGC 4531/56 pair with an exposure of 49^h5 (Fig. 1, see also <http://tbg.vdsastro.de>). This image reveals different signs of interaction between the components of this pair with a characteristic surface brightness of $29^m-30^m/\square''$. Some of them are indistinguishable from faint reflection nebulae. All the three objects dw1/2/3, according to their texture and location, are probably the physical satellites of NGC 4631. However, radial velocity measurements of these dwarfs are required to confirm this obvious assumption, which is a difficult observational task.

3.2. M 101 = NGC 5457

The spiral galaxy M 101, viewed face-on, is one of the most prominent representatives of the Local Volume population. The distance to it by the Cepheids is estimated as 7.38 Mpc [25], which happens to coincide with the distance to NGC 4631. According to [26], M 101 has six satellites, including an intergalactic HI cloud GBT 1355+5439 [27]. In 2009 and 2010 Mihos et al. [28] obtained deep images of the neighborhood of M 101 with the Burrell Schmidt telescope. The image mosaics covered a field sized $2^{\circ}5 \times 2^{\circ}5$ with the surface brightness limit $SB(B) \sim 29^m5/\square''$. The authors noted the presence in M 101 of two structural disturbances on the periphery: the northeastern spot and the eastern protrusion. However, they did not report a discovery of any new nearby satellites. In March 2012, a deep image of M 101 with an exposure of 40^h was obtained by F. Neyer using a telescope with a diameter of 15 cm and a focal ratio of $f/7.2$. The image size is $121' \times 80'$. The reproduction of the fragments of this image is shown in three panels of Fig. 2. In addition to the above-mentioned distortions of the periphery of M 101, on the northern and northeastern side the image reveals ten small LSB objects. All of them are located in the eastern half of the image with respect to M 101, which looks pretty mysterious.

In May–June 2013, van Dokkum et al. [29] and Merritt et al. [30] performed a survey of the neighborhood of M 101 using the Dragonfly Telephoto Array. This telescope is a robotic system of eight lenses, each one with a focal length of 40 cm and a focal ratio of $f/2.8$. This results in an effective aperture of 403 mm and the summed up focal ratio of about $f/1$. The field of view is $2^{\circ}6 \times 1^{\circ}9$ with a resolution of $2''8/\text{px}$. Given a total exposure of 35^h , the Dragonfly team reached a surface brightness limit $SB \sim 29^m5/\square''$. As a result, the authors found seven M 101 dwarf satellite candidates and designated them as DF1, DF2, ..., DF7. Six of them proved to be common with the objects in the image of F. Neyer, and one, DF5, is located outside the image field. At the same time, two LSB objects that we have designated as M 101 dwA and M 101 dwC were not noted by the Dragonfly team. The Dragonfly deep image limit allowed Merritt et al. [30] to conduct surface photometry of the detected objects and to determine their integrated g and r magnitudes, effective diameter, central surface

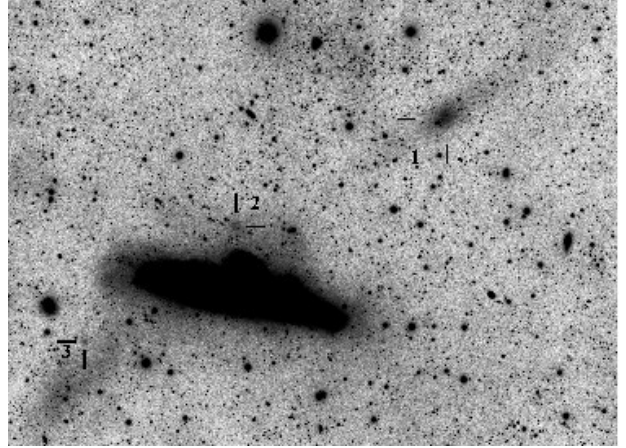


Figure 1. The galaxy NGC 4631 and three of its supposed companions, located along the diagonal tidal stripe. A $45' \times 33'$ fragment of an image obtained by F. Neyer with an exposure time of 49^h5 . North is at the top, east is to the left.

brightness, and the Sérsic structural index. Recently, M. Elvov obtained a broader image of the vicinity of M 101, where we found two more satellite candidates: M 101 dwB and M 101 dwD.

3.3. NGC 2683

This massive spiral galaxy at a distance of 9.36 Mpc [31] has two close and one distant satellite, KK 69, KK 70, and AGC 182595 respectively, the distances to which were measured with the Hubble Space Telescope [31, 32]. This poor group is located in the region of low galaxy number density on the front edge of the Gemini–Leo Void.

Two deep images centered on NGC 2683 were obtained by M. Elvov and G. Kerschhuber. The field sizes and exposures were $31' \times 22'$, $t = 15^h$ and $41' \times 55'$, $t = 12^h$ respectively. The reproduction of the second image fragment (Fig. 3) reveals two LSB dwarf objects, designated as dw1 and dw2. The brighter of them is identified with a UV source of the GALEX survey [33]. Its image in the $H\alpha$ line [34], taken with the 6-meter telescope of the Special Astrophysical Observatory of the Russian Academy of Sciences (SAO RAS) with the SCORPIO focal reducer [35], detects weak emission. The [O III], $H\beta$, and $H\gamma$ [36] emission lines are present in the spectrum of the object obtained with the same telescope [36]. Based on them, the heliocentric radial velocity of the object is $V_h = 380 \pm 25 \text{ km s}^{-1}$, which is close to the radial velocity of NGC 2683 itself,

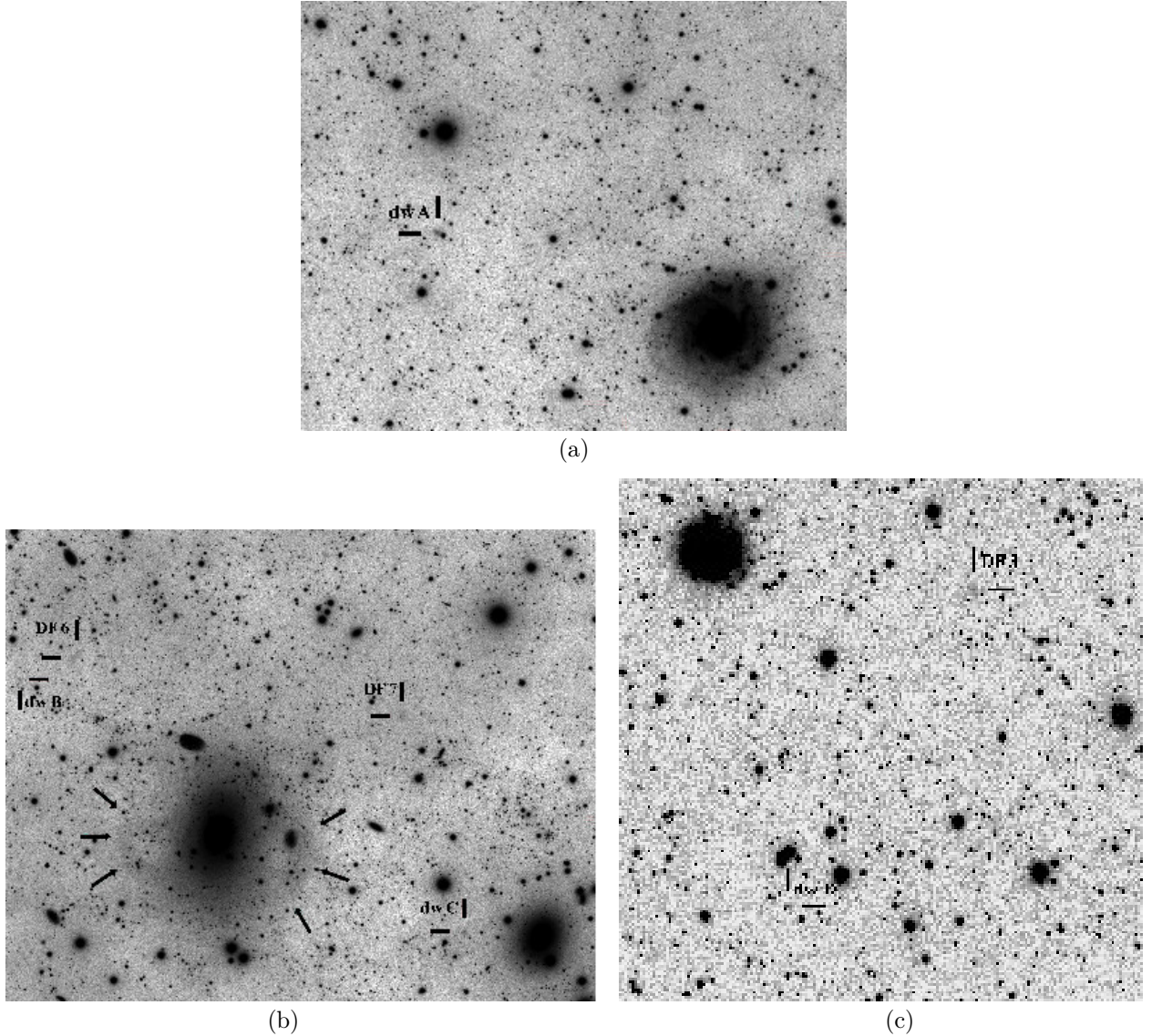


Figure 2. Fragments of the image displaying the neighborhood of M101, obtained by F. Neyer with an exposure of $45^{\text{h}}6$. (a) The region of an M101 satellite, the galaxy NGC 5477, and a new satellite candidate dwA; the frame size is $36' \times 24'$. (b) The area to the northeast of M101 sized $39' \times 31'$, in which the Dragonfly DF 6 and DF 7 objects and two new M101 satellite candidates dwB and dwC are located. Down from the center, a far background galaxy NGC 5485 is located (a distance of 28 Mpc), around which diffuse elliptical shells, shown by the arrows were detected for the first time. (c) A fragment of an image obtained by M. Elvov with an exposure of $11^{\text{h}}3$. In the area sized $34' \times 34'$, the NGC 5477 galaxy (the upper left corner), the Dragonfly DF 3 object, and a new M101 satellite candidate dwD are visible. In all the images north is at the top, and east is to the left.

$V_h = 411 \pm 4 \text{ km s}^{-1}$. The agreement of radial velocities indicates that the new dwarf galaxy is a real companion of NGC 2683. Low surface brightness of the second (dSph) dwarf galaxy makes its radial velocity measurement quite difficult.

3.4. NGC 891

According to [14], the entourage of the spiral galaxy NGC 891, seen edge-on, consists of four Sm and Irr galaxies: DDO 22, DDO 24, UGC 1807, and UGC 2172. The distance to the main galaxy, 9.77 Mpc, was determined from the surface brightness fluctuations [37]. The group itself is associated with the spiral galax-

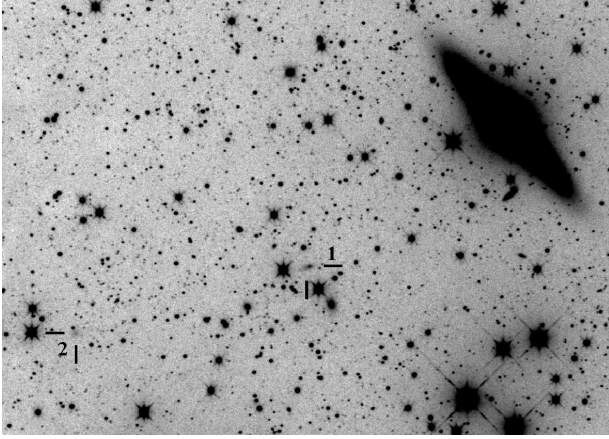
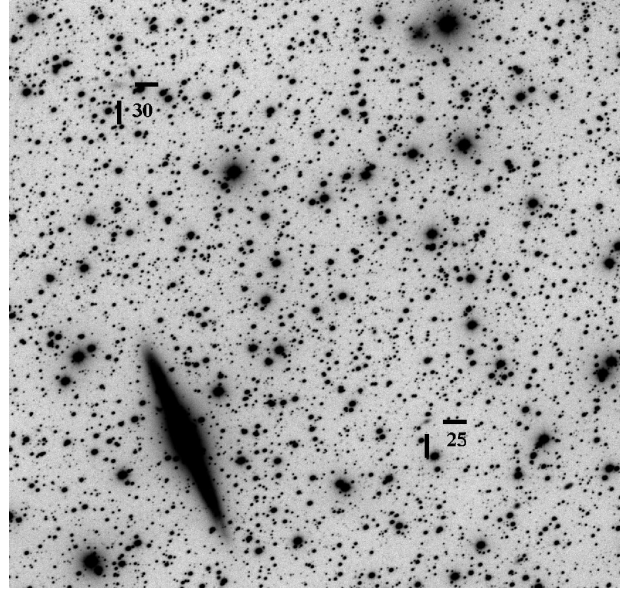


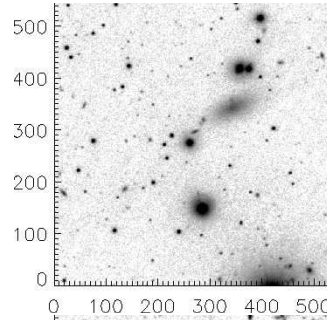
Figure 3. An image of the spiral galaxy NGC 2683 (in the upper right corner) and its two prospective satellites. The frame size is $29' \times 21'$. The image was obtained by G. Kerschhuber with an exposure of 12^{h} . Based on the measured radial velocity, the object “1” is a true satellite of NGC 2683.

ies NGC 925 and NGC 1023, forming a more extended and non-virialized complex.

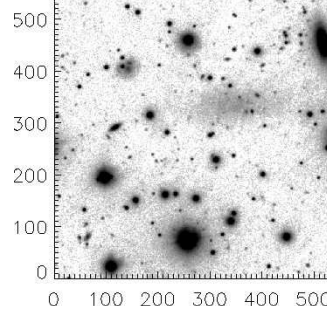
Faint satellites of NGC 891 were searched for by Trentham and Tully [38] and Schulz [39]. The former authors used broadband exposures with the MegaCam detector of the 3.6-m CFHT telescope. In the immediate surroundings of NGC 891, the authors found only two dwarf companion candidates: [TT 2009] 25 and [TT 2009] 30. Schulz [39] searched for new satellites of NGC 891 based on the data from various available surveys of the sky from the ultraviolet (GALEX) to the infrared (2MASS, WISE) range. Two out of seven suspected new satellites turned out to be already known, and the remaining five are likely to be the objects of distant background. A CCD image of the vicinity of NGC 891 obtained by M. Elvov on the 10-cm refractor ($f/5$) with an exposure of 12^{h} (Fig. 4a) detects the presence of two LSB dwarf galaxies dwA and dwB, which are identified with the objects [TT 2009] 25 and [TT 2009] 30. We have obtained large-scale images of both galaxies in the $\text{H}\alpha$ line and in the continuum (filter SED607) [31] with the SAO RAS 6-m telescope (Figs. 4b and 4c). They did not reveal any $\text{H}\alpha$ emission, even though in the GALEX survey they show weak FUV fluxes. For a brighter spheroidal galaxy [TT 2009] 25, a spectrum was obtained with the SAO RAS 6-m telescope [36]. Based on three absorption lines, the radial velocity of the galaxy is $V_h = 692 \pm 58 \text{ km s}^{-1}$, which is



(a)



(b)



(c)

Figure 4. (a) The spiral galaxy NGC 891 and its two dwarf satellites: dwA = [TT 2009] 25 and dwB = [TT 2009] 30. A $33' \times 32'$ fragment of an image obtained by M. Elvov with an exposure of 12^{h} . (b, c) Images of the dwarf galaxies [TT 2009] 25 and [TT 2009] 30, obtained by S. S. Kaisin on the SAO RAS 6-meter telescope with the SED607 filter with 1650-s and 2400-s exposures respectively. In all the images north is at the top, east is to the left.

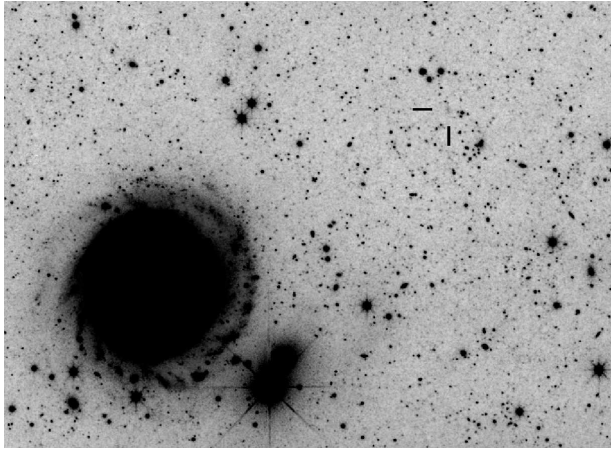


Figure 5. An image of the spiral galaxy NGC 3344 and its suspected dwarf companion NGC 3444 dw1, marked by arrows. The image was obtained by G. Kerschhuber and M. Blauensteiner based on simultaneous data from four telescopes with a total exposure of $28^{\text{h}}8$. The size of the fragment is $22' \times 16'$. North is at the top, east is to the left.

close to the heliocentric velocity of NGC 861 itself: $V_h = 526 \pm 7 \text{ km s}^{-1}$. According to the texture of the object [TT 2009] 30, it too, with a high probability, is a satellite of NGC 891.

3.5. NGC 3344 = KIG 435

This is an isolated galaxy seen face-on, with a regular spiral pattern. None of its physical satellites were known to date. An image of the surroundings of NGC 3344 made by Kerschhuber and Blauensteiner with a total exposure of $28^{\text{h}}8$ and field of $40' \times 30'$ reveals a suspected LSB satellite (Fig. 5) $12'$ northwest of NGC 3344. In this place, the SDSS survey [1] reveals a faint bluish spot with an angular size of $0'.3$. The GALEX survey did not detect this object.

3.6. NGC 4258 = M 106

A careful search for faint satellites around the spiral galaxy NGC 4258 was compiled by Kim et al. [40]. For this purpose, the authors used images taken with the CFHT telescope MegaCam detector, covering a field of $1.7^\circ \times 2.0^\circ$. They found sixteen M 106 satellite candidates and presented for them the surface photometry in the g and r bands. Two objects, S 11 and S 16,

proved to be new compared to the previous investigations of the M 106 neighborhood [41]. Later, Spencer et al. [42] made radial-velocity measurements of the suspected satellites of NGC 4258. This way they were trying to identify the physical satellites of NGC 4258 among the background galaxies. However, the M 106 group is located in a complicated region at the equator of the Local Supercluster. Next to it there are two more groups around the galaxies NGC 4346 and NGC 4157 with radial velocities close to that of M 106. The groups have average distance estimates of 16.4 Mpc and 17.5 Mpc respectively, forming the distant background for the NGC 4258 group ($D = 7.83$ Mpc by the Cepheid method).

The TBG group members obtained a few images of the neighborhood of M 106 with exposures ranging from 6^{h} to 20^{h} . In the area common with the field of view of [40], all the objects identified in [40] as suspected companions of M 106 were detected. Moreover, we have found a new LSB dwarf galaxy, indicated in Fig. 6 as dwA. As Dr. H. Ann reported to us, in their image made with MegaCam this object has not been noted, since it fell in the gap between two CCD chips. In addition, outside the MegaCam field of view we found two more LSB objects dwB and dwC, which look like very probable companions of M 106 (see <http://tbg.vdsastro.de>).¹

3.7. NGC 672/IC 1727

This tight pair of late-type spiral galaxies at a distance of 7.16 Mpc has three dwarf systems as its close satellites: KK 13, KK 14, and KK 15 [23]. In three images of the neighborhood of the pair obtained by the TBG members, we have selected four probable satellite candidates. They are marked on the three panels of Fig. 7 by the letters A, B, and C. Another candidate with the coordinates 014738.4+272620 is located

¹ Near the southern edge of Fig. 6, a distant background galaxy NGC 4217 is located. Its radial velocity $V_{\text{LG}} = 1084 \text{ km s}^{-1}$, and the distance, according to NED, is 19.3 Mpc. On the northeastern edge of NGC 4217, a round LSB feature is visible, which may be a tidal bulge in the disk of the spiral. If, however, this is a dwarf companion of NGC 4258, projected on the outskirts of NGC 4217, then its absolute magnitude $M_B = -11.5$, its linear diameter is 2.5 kpc, and the mean surface brightness $\text{SB} = 26^{\text{m}}8/\square''$.

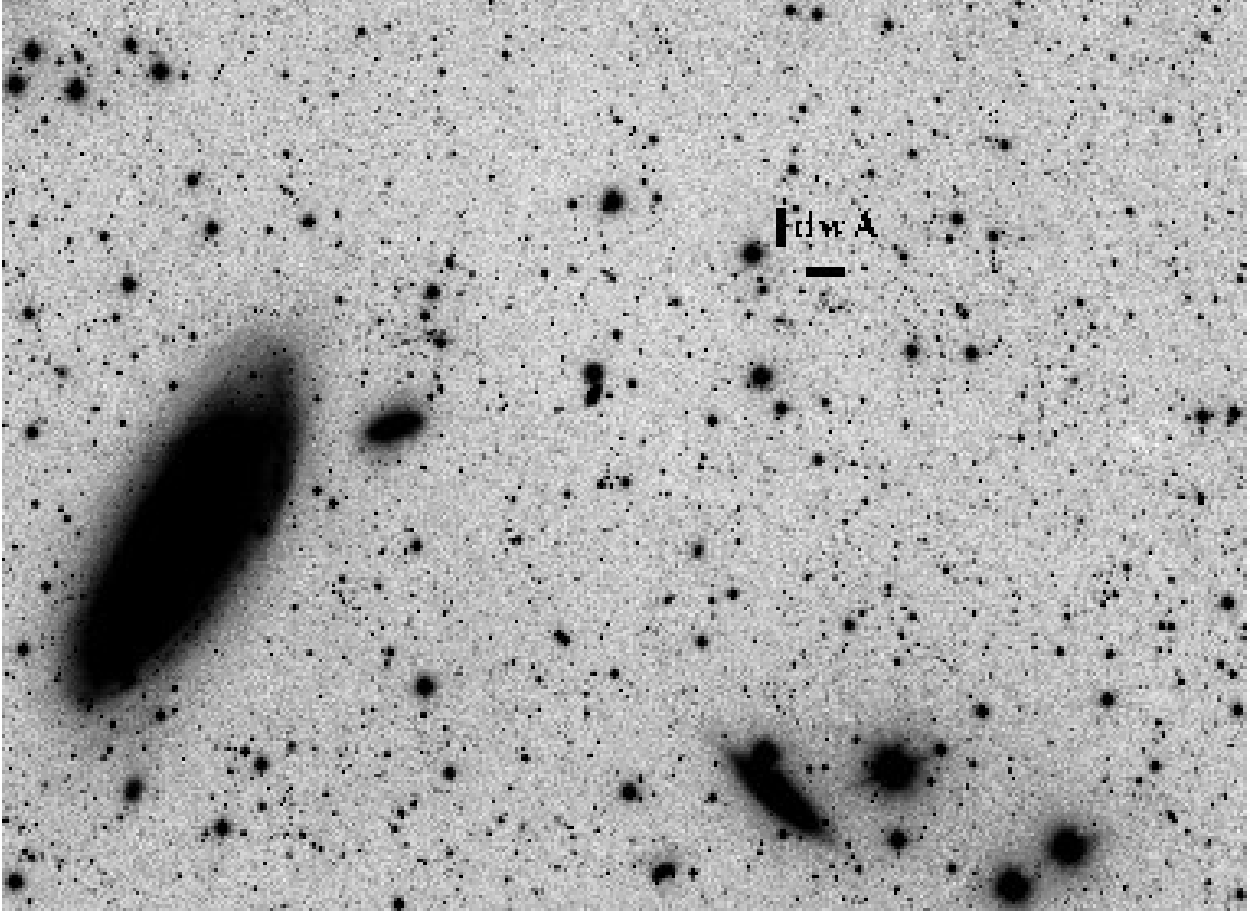


Figure 6. The spiral galaxy NGC 4258 = M 106 and its new suspected satellite NGC 4258 dwA. The image was obtained by M. Elvov with a 20-h exposure. The reproduced part of the image is $65' \times 48'$. North is at the top, east is to the left.

in contact with NGC 672, and is the brightest ($B = 18^m7$) and the most compact. We have obtained its spectrum with the SAO RAS 6-meter telescope. The velocity of the object proved to be very large, $V_h = 29860 \pm 110 \text{ km s}^{-1}$ [36], and we excluded it from the group. Three other LSB galaxies look more like close dwarfs. Radial-velocity measurements are required to confirm their membership in the NGC 672 group.

3.8. NGC 4618/NGC 4625

This is a pair of dwarf spirals at a distance of 7.9 Mpc with a radial velocity difference of 70 km s^{-1} . The spiral structure is distorted in both galaxies, which indicates their interaction. An Im-type dwarf galaxy UGC 7751 is associated with this pair, and possibly another, fainter irregular dwarf LV J1243+4127 too [12]. Investigating an extended ultra-

violet disk around NGC 4625, Gil de Paz et al. [43] noted the presence $4'$ east of it of an LSB object, which they named NGC 4625 A. The reproduction of an image of the NGC 4618/25 pair and the dwarf galaxy NGC 4625 A obtained by R. Sparenberg is shown in Fig. 8. We have included NGC 4625 A in the list of objects for measuring radial velocities, assuming that it can prove to be a physical companion of the NGC 4618/25 pair.

3.9. NGC 1156 = KIG 121

This isolated Magellanic type dwarf galaxy with an apparent magnitude $B = 12^m3$ and radial velocity $V_h = 373 \text{ km s}^{-1}$ is located in the zone of significant ($A_b = 0^m97$) Galactic extinction. The image of its surroundings with a $46' \times 34'$ field of view was obtained by P. Hochleitner on a 36 cm diameter telescope with an expo-

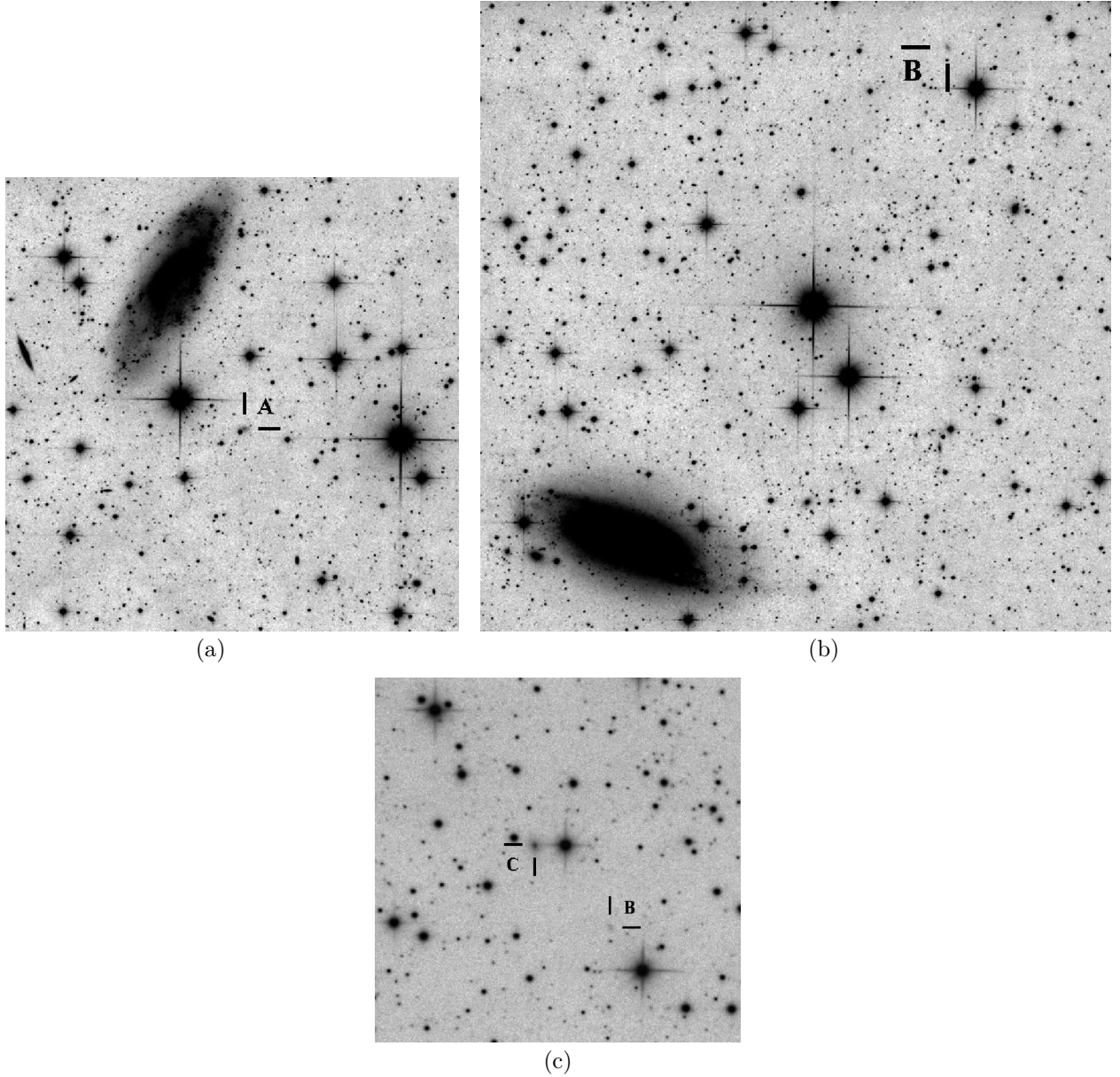


Figure 7. (a) The galaxy IC 1727 and the dwarf galaxy N 672 dwA (a $14' \times 14'$ part of an image obtained by R. Pöelz with an exposure of 21^{h}). (b) The galaxy NGC 672 and its assumed satellite dwB (a $19' \times 19'$ fragment of the same image by R. Pözl). (c) The area to the north of NGC 672 with its two supposed satellites NGC 672 dwB and NGC 672 dwC (a $10' \times 10'$ fragment of an image obtained by S. Küppers with an exposure of $5^{\text{h}}3$). In all the images north is at the top, east is to the left.

sure of 11^{h} . Reflection nebulae (cirri), the presence of which imposes a limit on the detection of LSB galaxies, are seen almost over the entire area of the image. Nevertheless, two LSB objects, dw1 and dw2, which can be classified as satellites of NGC 1156, are present in the image (Fig. 9). The first one of them is located in the halo of a bright star SAO 75679. Both objects are barely discernible in the photographic sky survey DSS2.

Note that the vicinity of NGC 1156 was investigated by Minchin et al. [44] within the deep HI AGES survey using the Arecibo radio telescope. These observations led to the discovery of an irregular dwarf galaxy AGES J030039+254656 with a radial velocity $V_h = 308 \text{ km s}^{-1}$ and apparent magnitude $B = 18^{\text{m}}1$, which is located to the north, beyond the scope of our image. Two NGC 1156 satellite candidates that we have discovered look about two magnitudes fainter than

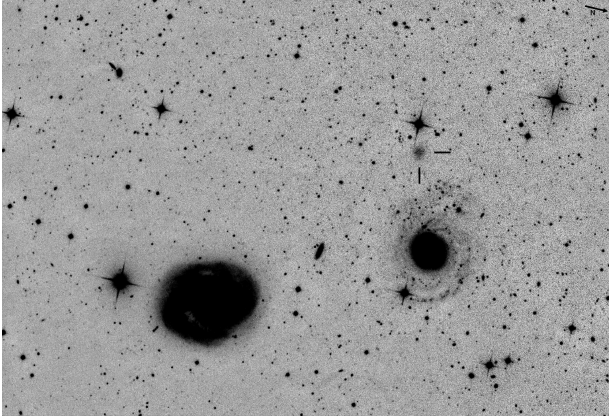


Figure 8. An interacting pair of galaxies NGC 4618 (left) and NGC 4625, and a dwarf galaxy NGC 4626 A, marked by the arrows. A $23' \times 16'$ fragment of an image obtained by R. Sparenberg on a 44-inch telescope with an exposure of $3^{\text{h}}5$. The arrow in the upper right corner indicates the north direction.

the AGES satellite. Obviously, their HI fluxes could be below the AGES survey limit.

3.10. NGC 2903, NGC 3239, NGC 4214, NGC 5585

Apart from the nine galaxies mentioned above, we have obtained long-exposure images for four other galaxies in the Local Volume. However, the search for new candidate satellites of these galaxies proved to be unsuccessful.

The massive spiral galaxy NGC 2903 is listed in the catalog of isolated galaxies [45]. Although it has four tiny satellites, due to their small size this is not inconsistent with the catalog isolation criterion. Just like in the case of NGC 2683, this galaxy is on the front edge of the nearby Gemini–Leo Void, whose center lies about 18.4 Mpc from us, and whose radius is 7.5 Mpc. Deep images of the vicinity of NGC 2903 made by M. Blaustein, M. Elvov, and S. Küppers did not reveal any new companion candidates of the massive spiral.

An interactive pair of merging galaxies NGC 3239 = Arp 263 = VV 095 contains a scattering of star formation centers. Two curved tails extending to the south of the main body of the galaxy make it similar to the Greek letter “ π .” Around this violently interacting system one would expect to find a multitude of small irregular satellites formed by the fragmentation of tidal tails. However, they have not been found

in the image made by B. Hubl with an exposure of 32^{h} .

A magellanic-type dwarf galaxy NGC 4214 at a distance of 2.94 Mpc [13] is in the stage of violent star formation. Next to it there is a dwarf spheroidal galaxy KDG 90, the distance to which, 2.86 Mpc [13], indicates the physical connection with NGC 4214. However, the images obtained by G. Willems and G. Kerschhuber with an exposure of $19^{\text{h}}1$ do not show any obvious signs of mutual perturbations in these galaxies, apart from a faint diffuse protrusion on the southwestern periphery of NGC 4214. No new NGC 4214 satellite candidates have either been found.

A dwarf Sm spiral NGC 5585 at a distance of 5.7 Mpc is a distant satellite of a giant spiral M 101. The periphery of the galaxy looks quite regular, without disturbances. The image obtained by B. Hubl with an exposure of 15^{h} did not reveal any satellite candidates of this galaxy in the $30' \times 30'$ field. The reproductions of the said images and the comments to them can be found on <http://tbg.vdsastro.de>.

4. DISCUSSION

The main features of the thirteen nearby spiral galaxies that we have observed with long exposures are presented in Table 1. Its columns contain: (1) the names of the galaxies, ranked by right ascension; (2) the coordinates of the galaxy for the epoch J2000.0; (3) the morphological type according to de Vaucouleurs’ scale; (4) the radial velocity in km s^{-1} relative to the centroid of the Local Group; (5) the distance to the galaxies in Mpc and the applied method of distance determination: “cep”—the Cepheid luminosity method, “rgb”—by the luminosity of red giant branch stars, “sbf”—by surface brightness fluctuations, “tf”—by the Tully–Fisher relation between the amplitude of rotation of a galaxy and its luminosity, “bs”—by the luminosity of the brightest stars; (6) the absolute magnitude of the galaxy in the B band adjusted for the Galactic [46] and internal extinction; (7) the linear Holmberg diameter of the galaxy in kpc; (8, 9) the logarithm of the stellar mass and the mass of neutral hydrogen in solar mass units; (10) the logarithm of the stellar mass density within the 1 Mpc radius sphere around the galaxy, taken in relation to the average cosmic stellar mass density; (11) the number of known satellites of the galaxy within the “zero-velocity radius” sphere around it plus

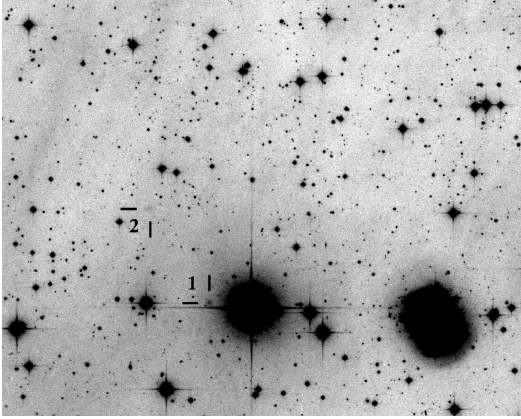


Figure 9. An isolated galaxy NGC 1156 in the lower right corner and two of its suspected satellites dw1 and dw2. A $19' \times 15'$ fragment of an image obtained by P. Hochleitner with an exposure of 11^{h} . North is at the top, east is to the left.

the number of new satellite candidates that we found and discussed above; (12) the signs of disturbances on the periphery of the galaxy if any of them can be seen in our deep images.

Most of the Table 1 data are taken from the UNGC [13], which gives evaluations of the parameters used. Some distance estimates have been updated with recent observations of the Hubble Space Telescope.

Despite the small statistics, the Table 1 data show the presence of a positive correlation between the luminosity of a galaxy (its linear diameter, mass) and the number of satellites around it. The average density of the environment also affects the amount of physical satellites. For example, two galaxies in the region of a cosmic void, NGC 2683 and NGC 2903, have six satellites and two new candidates, while the two galaxies in the dense environment, NGC 4258 and NGC 4631 with approximately the same luminosity, have twenty-four physical satellites and six new candidates. The noted trends suggest near which galaxies there is a chance to find the greatest number of new satellites during a further search.

The distant periphery of Andromeda-type massive galaxies preserves in itself in the form of faint stellar streams relic signs of interaction with neighbors or traces of the capture of satellites which happened a few billion years ago. The last column of Table 1 provides indications on the possible events of this kind in the history of thirteen nearby high luminosity galaxies.

A summary of the data on twenty-seven detected satellite candidates of the thirteen nearby

spiral galaxies is given in Table 2. Its columns contain: (1) the name of the dwarf galaxy; (2) the galaxy coordinates for the epoch 2000.0; (3) the morphological type of the dwarf: irregular (Ir), spheroidal (Sph), or transition (Tr), with a visual estimation of surface brightness: low (L), very low (VL), or extremely low (XL); (4) the apparent B magnitude estimated by eye via comparing with other dwarf objects of similar structure and known photometry; in some of the brightest objects the B magnitude is determined from the SDSS survey g and r magnitudes, the measure of inaccuracy of our estimates is about $0^{\text{m}}5$; (5) the maximum apparent angular diameter a in arcminutes; (6) the surface brightness $\text{SB} = B^c + 5 \log a' + 8.63$ in magnitudes per square arcsecond, where the B magnitude is corrected for the Galactic extinction; (7, 8) the projected distance of the satellite from the main galaxy in arcminutes and in kpc; (9, 10) the absolute magnitude and linear diameter of the satellite; (11) whether the object has a FUV flux from the GALEX survey or an alias. The last line of the table shows the average values of the above parameters.

We can see from these data that the absolute magnitudes of the suspected new satellites around nearby spirals are confined in the range from $-8^{\text{m}}6$ to $-13^{\text{m}}3$ with an average value of $-10^{\text{m}}4$. Linear diameters of the satellites lie in the range from 0.4 kpc to 4.7 kpc with an average of 1.3 kpc. The range of both parameters is typical for the dwarf satellites of M 31 and M 81. The average surface brightness of the discovered dwarfs $\langle \text{SB} \rangle = 26^{\text{m}}1/\square''$ barely exceeds the Holmberg isophote brightness of $26^{\text{m}}5/\square''$, which is the detection limit for low-contrast objects observed with photographic emulsions.

The average projected separation of new satellites from their host galaxies is 73 kpc. This value is 3–4 times smaller than the characteristic radius of an entourage of dwarfs around a Milky Way-type massive galaxy. It is obvious that such a difference is due to the small field of view of the used telescopes, which is comparable to the average angular separation of the satellites $\langle r_p \rangle = 32'.4$. It hence follows that a significant number of low and very low surface brightness dwarf satellites can still be found around massive Local Volume galaxies in the field of view with a radius of 1° – 2° . However, their search would require a lot more observing time of the telescopes in use or attraction of new astronomical CCD imaging enthusiasts to this program.

5. CLOSING REMARKS

Detection of ultra-faint dwarf satellites around nearby massive galaxies is of important cosmological significance. Successful search for such objects in the Local Group around the Milky Way and the Andromeda Nebula (M31) attracted great interest to the features of their spatial distribution and kinematics [47–49].

Many believe that ultra-faint dwarf galaxies are among the “darkest” objects in the Universe and in this sense they can serve as a natural laboratory to study the nature of dark matter.

The program of detection of faint dwarf galaxies with small telescopes should obviously be accompanied by systematic radial velocity measurements of new LSB objects to confirm their physical connection with massive galaxies. Radial velocity measurements as well as the studies of the photometric structure of new dwarf galax-

ies require the capabilities of large telescopes. It remains to add that extending the program to the southern sky objects is a quite evident and topical task.

ACKNOWLEDGMENTS

The authors are grateful to S. S. Kaisin, D. I. Makarov, M. E. Sharina, Yu A. Perepelitsyna, and E. S. Safonova, who took part in the observations at the 6-m telescope and data processing. This work was supported by Russian Science Foundation grant No. 14-12-00695. Observations on the 6-m telescope of the Special Astrophysical Observatory are held with financial support from the Ministry of Education and Science of the Russian Federation (contract No. 14.619.21.0004, project identifier RFMEFI61914X0004).

-
1. K. N. Abazajian, J. K. Adelman-McCarthy, M. A. Agueros, et al., *Astrophys. J. Suppl.***182**, 543 (2009).
 2. R. Giovanelli, M. P. Haynes, B. R. Kent, et al., *Astronom. J.***130**, 2598 (2005).
 3. M. P. Haynes, R. Giovanelli, A. M. Martin, et al., *Astronom. J.***142**, 170 (2011).
 4. T. H. Jarrett, T. Chester, R. Cutri, et al., *Astronom. J.***119**, 2498 (2000).
 5. T. H. Jarrett, T. Chester, R. Cutri, et al., *Astronom. J.***125**, 525 (2003).
 6. B. S. Koribalski, L. Staveley-Smith, V. A. Kilborn, et al., *Astronom. J.***128**, 16 (2004).
 7. M. A. Zwaan, L. Staveley-Smith, B. S. Koribalski, et al., *Astronom. J.***125**, 2842 (2003).
 8. K. Kovač, T. A. Oosterloo, and J. M. van der Hulst, *Monthly Notices Roy. Astronom. Soc.***400**, 743 (2009).
 9. J. L. Tonry, C. W. Stubbs, K. R. Lykke, et al., *Astrophys. J.* **750**, 99 (2012).
 10. V. E. Karachentseva and I. D. Karachentsev, *Astronom. and Astrophys. Suppl. Ser.***127**, 409 (1998).
 11. V. E. Karachentseva and I. D. Karachentsev, *Astronom. and Astrophys. Suppl. Ser.***146**, 359 (2000).
 12. W. K. Huchtmeier, I. D. Karachentsev, and V. E. Karachentseva, *Astronom. and Astrophys.***506**, 677 (2009).
 13. I. D. Karachentsev, D. I. Makarov, and E. I. Kaisina, *Astronom. J.***145**, 101 (2013).
 14. E. I. Kaisina, D. I. Makarov, I. D. Karachentsev, and S. S. Kaisin, *Astrophysical Bulletin***67**, 115 (2012).
 15. B. Moore, S. Ghigna, F. Governato, et al., *Astrophys. J.* **524**, L19 (1999).
 16. A. Klypin, A. V. Kravtsov, O. Valenzuela, and F. Prada, *Astrophys. J.* **522**, 82 (1999).
 17. R. Ibata, N. F. Martin, M. Irwin, et al., *Astrophys. J.* **671**, 1591 (2007).
 18. R. A. Ibata, G. F. Lewis, A. R. Conn, et al., *Nature*, **493**, 62 (2013).
 19. N. F. Martin, A. W. McConnachie, M. Irwin, et al., *Astrophys. J.* **705**, 758 (2009).
 20. K. Chiboucas, I. D. Karachentsev, and R. B. Tully, *Astronom. J.***137**, 3009 (2009).
 21. K. Chiboucas, B. A. Jacobs, R. B. Tully, and I. D. Karachentsev, *Astronom. J.***146**, 126 (2013).
 22. D. J. Radburn-Smith, R. S. de Jong, A. C. Seth, et al., *Astrophys. J. Suppl.***195**, 18 (2011).
 23. I. D. Karachentsev, D. Bautzmann, F. Neyer, et al., arXiv:1401.2719.
 24. D. Martinez-Delgado, E. D’Onghia, T. S. Chonis, et al., arXiv:1410.6368.
 25. L. Ferrarese, H. C. Ford, J. Huchra, et al. *Astrophys. J. Suppl.***128**, 431 (2000).
 26. I. D. Karachentsev, E. I. Kaisina, and D. I. Makarov, *Astronom. J.***147**, 13 (2014).
 27. J. C. Mihos, K. M. Keating, K. Holley-Bockelmann, et al., *Astrophys. J.* **761**, 186 (2012).

28. J. C. Mihos, P. Harding, C. E. Spengler, et al., *Astrophys. J.* **762**, 82 (2013).
29. P. G. van Dokkum, R. Abraham, and A. Merritt, *Astrophys. J.* **782**, 24 (2014).
30. A. Merritt, P. van Dokkum, and R. Abraham, *Astrophys. J.* **787**, L37 (2014).
31. I. D. Karachentsev, R. B. Tully, L. N. Makarova, et al., *Astrophys. J.* **805**, 144 (2015).
32. K. B. W. McQuinn, J. M. Cannon, A. E. Dolphin, et al., *Astrophys. J.* **785**, 3 (2014).
33. A. Gil de Paz, S. Boissier, B. F. Madore, et al., *Astrophys. J. Suppl.* **173**, 185 (2007).
34. I. D. Karachentsev, S. S. Kaisin, and E. I. Kaisina, *Astrophysics*, **58**, 331 (2015).
35. V. L. Afanasiev and A. V. Moiseev, *Astron. Lett* **31**, 194 (2005).
36. I. D. Karachentsev, M. E. Sharina, D. I. Makarov, et al., *Astrophysics*, **58** (2015) (in press).
37. L. Ferrarese, J. R. Mould, R. C. Kennicutt, et al., *Astrophys. J.* **529**, 745 (2000).
38. N. Trentham N. and R. B. Tully, *Monthly Notices Roy. Astronom. Soc.* **398**, 722 (2009).
39. E. Schulz, *Astrophys. J.* **790**, 76 (2014).
40. E. Kim, M. Kim, N. Hwang, et al., *Monthly Notices Roy. Astronom. Soc.* **412**, 1881 (2011).
41. I. D. Karachentsev, V. E. Karachentseva, and W. K. Huchtmeier, *Astron. Lett.* **33**, 512 (2007).
42. M. Spencer, S. Loebman, and P. Yoachim, *Astrophys. J.* **788**, 146 (2014).
43. A. Gil de Paz, B. F. Madore, S. Boissier, et al., *Astrophys. J.* **627**, L29 (2005).
44. R. F. Minchin, E. Momjian, R. Auld, et al., *Astronom. J.* **140**, 1093 (2010).
45. V. E. Karachentseva, *Soobschenia SAO*, No. 8, 3 (1973).
46. D. J. Schlegel, D. P. Finkbeiner, and M. Davis, *Astrophys. J.* **500**, 525 (1998).
47. P. Kroupa, C. Theis, and C. M. Boily, *Astronom. and Astrophys.* **431**, 517 (2005).
48. R. A. Ibata, G. F. Lewis, A. R. Conn, et al., *Nature*, **493**, 62 (2013).
49. E. J. Shaya and R. B. Tully, *Monthly Notices Roy. Astronom. Soc.* **436**, 2096 (2013).

Table 1. Nearby massive galaxies observed by the TBG group

| Name | RA (2000.0) Dec | T | V_{LG} , km s^{-1} | D , Mpc; method | M_B , mag | A_H , kpc | $\log M^*$, $[M_\odot]$ | $\log M_{HI}$, $[M_\odot]$ | Θ_j | N_{sat} | Periphery shape |
|----------|-----------------|-----|----------------------------------|----------------------|----------------|----------------|-----------------------------|--------------------------------|------------|------------------|--------------------|
| (1) | (2) | (3) | (4) | (5) | (6) | (7) | (8) | (9) | (10) | (11) | (12) |
| NGC 672 | 014753.2+272601 | 6 | 626 | 7.16 rgb | -18.76 | 15.7 | 10.22 | 9.23 | 0.2 | 3+3 | regular |
| NGC 891 | 022232.8+422048 | 3 | 736 | 9.97 sbf | -20.58 | 38.7 | 10.98 | 9.66 | -0.1 | 4+2 | regular |
| NGC 1156 | 025942.4+251415 | 8 | 507 | 7.80 bs | -18.14 | 9.2 | 9.31 | 8.82 | -1.5 | 1+2 | NE extention |
| NGC 2683 | 085240.9+332502 | 3 | 365 | 9.36 rgb | -20.78 | 35.7 | 10.76 | 9.10 | -1.4 | 2+2 | regular |
| NGC 2903 | 093209.6+213002 | 4 | 443 | 8.87 bs | -20.89 | 32.4 | 10.82 | 9.44 | -0.8 | 4+0 | regular |
| NGC 3239 | 102504.9+170949 | 8 | 623 | 7.90 tf | -18.09 | 11.6 | 9.52 | 8.89 | -0.9 | 0+0 | faint halo |
| NGC 3344 | 104330.2+245525 | 4 | 500 | 9.83 rgb | -19.72 | 22.2 | 10.33 | 9.44 | -0.8 | 0+1 | regular? |
| NGC 4214 | 121538.9+361939 | 8 | 295 | 2.94 rgb | -17.20 | 7.3 | 9.00 | 8.48 | -0.7 | 3+0 | SSW protrusion? |
| NGC 4258 | 121857.5+471814 | 4 | 506 | 7.83 cep | -21.20 | 41.5 | 10.94 | 9.64 | 1.0 | 19+3 | twisted |
| NGC 4618 | 124132.8+410903 | 6 | 576 | 7.90 tf | -18.33 | 9.7 | 9.65 | 8.90 | 0.5 | 2+1 | N, E protrusions |
| NGC 4631 | 124208.0+323229 | 7 | 581 | 7.38 rgb | -20.28 | 33.7 | 10.49 | 9.72 | 1.0 | 5+3 | tails |
| M101 | 140312.8+542102 | 6 | 378 | 7.38 cep | -21.12 | 65.2 | 10.85 | 9.91 | 0.2 | 6+10 | asymmetric |
| NGC 5585 | 141948.3+564349 | 7 | 457 | 5.70 bs | -17.81 | 9.7 | 9.03 | 8.82 | -3.0 | 0+0 | regular |

Table 2. New LSB satellite candidates around nearby massive galaxies

| Name | RA (2000.0) Dec | T | B , mag | a , arcmin | SB | r_p , arcmin | R_p , kpc | M_B , mag | A , kpc | Note |
|--------------|-----------------|--------|--------------|-----------------|------|-------------------|----------------|----------------|--------------|----------|
| (1) | (2) | (3) | (4) | (5) | (6) | (7) | (8) | (9) | (10) | (11) |
| NGC 672 dwB | 014711.1+274100 | Ir-VL | 21.0 | 0.20 | 25.8 | 17.7 | 37 | -8.6 | 0.42 | |
| NGC 672 dwA | 014719.1+271516 | Ir-L | 19.8 | 0.26 | 25.2 | 13.1 | 27 | -9.8 | 0.54 | GALEX |
| NGC 672 dwC | 014720.4+274324 | Sph-L | 18.7 | 0.40 | 25.0 | 18.9 | 39 | -10.9 | 0.83 | |
| NGC 891 dwA | 022112.4+422150 | Tr-L | 17.9 | 0.76 | 25.7 | 14.9 | 43 | -12.3 | 2.20 | [TT09]25 |
| NGC 891 dwB | 022254.7+424245 | Ir-VL | 18.9 | 1.16 | 27.6 | 22.4 | 65 | -11.3 | 3.36 | [TT09]30 |
| NGC 1156 dw1 | 030018.2+251456 | Ir-L | 19.6 | 0.38 | 25.2 | 8.1 | 18 | -10.8 | 0.86 | |
| NGC 1156 dw2 | 030028.0+251817 | Ir-VL | 20.0 | 0.38 | 25.6 | 11.1 | 25 | -10.4 | 0.86 | GALEX |
| NGC 2683 dw1 | 085326.8+331820 | Ir-L | 19.0 | 0.40 | 25.5 | 11.7 | 32 | -11.0 | 1.09 | GALEX |
| NGC 2683 dw2 | 085420.5+331458 | Sph-VL | 19.6 | 0.40 | 26.1 | 23.1 | 63 | -10.4 | 1.09 | |
| NGC 3344 dw1 | 104244.0+250130 | Ir-VL | 20.0 | 0.30 | 26.0 | 11.9 | 34 | -10.1 | 0.86 | |
| NGC 4258 dwC | 121026.8+464449 | Sph-L | 19.0 | 0.27 | 24.7 | 93.3 | 212 | -10.5 | 0.61 | |
| NGC 4258 dwA | 121551.0+473256 | Ir-L | 19.0 | 0.43 | 25.7 | 34.8 | 79 | -10.5 | 0.98 | |
| NGC 4258 dwB | 122410.9+470723 | Sph-L | 18.3 | 0.45 | 25.1 | 54.6 | 124 | -11.2 | 1.02 | BTS134 |
| NGC 4631 dw1 | 124057.0+324733 | Ir-VL | 16.1 | 2.20 | 26.4 | 21.3 | 46 | -13.3 | 4.72 | GALEX |
| NGC 4631 dw2 | 124206.8+323715 | Ir-VL | 18.5 | 0.90 | 26.8 | 4.8 | 10 | -10.9 | 1.93 | GALEX |
| NGC 4625 A | 124211.0+411510 | Tr-L | 18.6 | 0.45 | 25.4 | 9.4 | 22 | -11.0 | 1.03 | |
| NGC 4631 dw3 | 124252.5+322735 | Sph-VL | 19.7 | 0.60 | 27.1 | 10.6 | 23 | -9.7 | 1.29 | |
| M 101 DF3 | 140305.7+533656 | Sph-VL | 17.9 | 1.00 | 26.5 | 44.1 | 95 | -11.5 | 2.15 | |
| M 101 DF1 | 140345.0+535640 | Ir-L | 18.9 | 0.47 | 25.8 | 23.9 | 51 | -10.5 | 1.01 | |
| M 101 dwD | 140424.6+531619 | Sph-VL | 19.2 | 0.38 | 25.7 | 65.6 | 141 | -10.2 | 0.81 | |
| M 101 dwC | 140518.0+545356 | Tr-VL | 20.2 | 0.30 | 26.2 | 37.6 | 81 | -9.2 | 0.64 | |
| M 101 DF7 | 140548.3+550758 | Sph-XL | 20.4 | 0.67 | 28.1 | 52.0 | 117 | -9.0 | 1.44 | |
| M 101 dwA | 140650.2+534432 | Sph-L | 19.2 | 0.36 | 25.6 | 45.3 | 97 | -10.2 | 0.77 | |
| M 101 DF4 | 140733.4+544236 | Ir-XL | 18.8 | 0.93 | 27.2 | 43.5 | 93 | -10.6 | 1.99 | |
| M 101 DF6 | 140819.0+551124 | Ir-XL | 20.1 | 0.73 | 28.0 | 67.2 | 144 | -9.3 | 1.57 | |
| M 101 DF2 | 140837.5+541931 | Sph-L | 19.8 | 0.33 | 26.0 | 47.1 | 101 | -9.6 | 0.71 | |
| M 101 dwB | 140843.1+550957 | Sph-VL | 20.1 | 0.30 | 26.1 | 68.0 | 146 | -9.3 | 0.64 | |
| Mean | | | 19.2 | 0.57 | 26.1 | 32.4 | 73 | -10.4 | 1.31 | |